Colloids and Surfaces B: Biointerfaces 109 (2013) 228–235

Contents lists available at SciVerse ScienceDirect

Colloids and Surfaces B: Biointerfaces

journal homepage: www.elsevier.com/locate/colsurfb

Physicochemical and biological evaluation of poly(ethylene glycol) methacrylate grafted onto poly(dimethyl siloxane) surfaces for prosthetic devices

Sara Gonçalves[a], Ana Leirós[a], Theo van Kooten[b], Fernando Dourado[a], Lígia R. Rodrigues[a,*]

[a] IBB-Institute for Biotechnology and Bioengineering, Centre of Biological Engineering, University of Minho, Campus de Gualtar, 4710-057 Braga, Portugal
[b] Department of Biomedical Engineering (BME), University Medical Center of Groningen, A. Deusinglaan 1, 9713 AV Groningen, The Netherlands

ARTICLE INFO

Article history:
Received 24 October 2012
Received in revised form 21 March 2013
Accepted 27 March 2013
Available online 9 April 2013

Keywords:
Poly(dimethyl siloxane)
Surface-initiated atom transfer radical polymerization
Anti-adhesion
Cytotoxicity

ABSTRACT

Poly(dimethyl siloxane) (PDMS) was surface-polymerized with poly(ethylene glycol)methacrylate (PEGMA) by surface-initiated atom transfer radical polymerization (SI-ATRP) in aqueous media at room temperature. Modification of the PDMS surface followed a three-step procedure: (i) PDMS surface hydroxylation by UV/ozone exposure, immediately followed by (ii) covalent attachment of the initiator, 1-trichlorosilyl-2-(chloromethylphenyl)ethane, onto the hydroxylated PDMS, *via* chemical vapor deposition; finally (iii) PDMS surface-polymerization of PEGMA by ATRP. Modified PDMS was characterized by water contact angle measurement, SEM, FTIR-ATR, and XPS. Results showed that modified surfaces had a hydrophilic character, given the water contact angles around 60°; FTIR-ATR and XPS analysis confirmed the presence of polymerized PEGMA on the surface of PDMS and the adhesion of *Staphylococcus aureus* GB 2/1 and *Streptococcus salivarius* GB 24/9 onto the modified surfaces was inhibited 94% and 81%, respectively. Finally, the modified PDMS showed no evidence of cytotoxic effects in *in vitro* assays using human skin fibroblasts.

1. Introduction

Prosthetic devices have been widely used to compensate for defects either from congenital or acquired origin (such as disease or trauma). Silicone (poly(dimethyl siloxane); PDMS) elastomers are well-known materials for the production of prosthesis. However, given their low surface-free energy (hence poor wettability), they can cause adverse reactions such as tissue irritation, abrasion and ulceration [1–5]. Additionally, PDMS surfaces are hydrophobic and highly prone to bacterial colonization. PDMS-associated implant infections often occur, mainly caused by *Staphylococcus* spp. and other Gram-positive bacteria [6–8]. A competition between integration of the material into the surrounding tissue and adhesion of bacteria to the implant surface occurs upon implantation [9]. For a successful implant, tissue integration, which is dictated by the material biocompatibility (non-cytotoxic), should occur prior to considerable bacterial adhesion. A 6 h post-implantation period has been identified during which prevention of bacterial adhesion is critical to the long-term success of an implant [10]. Over this period, an implant is particularly susceptible to surface colonization and any strategy that can limit bacterial adhesion is expected to have an impact in the further performance of the implant [11]. Therefore, modification of PDMS surfaces toward hydrophilic surfaces (less susceptible to bacterial adhesion) is a promising approach to reach a more generalized application of a material that is already extensively used for manufacturing implantable medical devices.

The central strategy to minimize the problems associated with PDMS and thus improve its clinical performance is to modify the surface properties of the elastomers, while allowing the material to retain its bulk properties. A body of literature already exists demonstrating the applications of physical, chemical and combinations of both methods for the surface modifications of PDMS polymers (reviews [12,13] cover these topics). An anti-adhesive surface can be obtained by modification with hydrophilic polymers. Polyethylene glycols (PEGs), a family of water-soluble polymers containing a common chemical structure, are widely known to resist non-specific protein adsorption and microbial adhesion, a property most likely to result from its hydrophilicity, a large excluded volume and a distinct ability to coordinate with surrounding water molecules [14,15].

In previous studies biosurfactants from probiotic bacteria were shown to inhibit the adhesion of bacterial and yeast strains on PDMS substrates [11,16,17]. This work undertakes an exploratory approach in the use of surface-initiated atom transfer radical

* Corresponding author. Tel.: +351 253604401; fax: +351 253604429.
E-mail address: lrmr@deb.uminho.pt (L.R. Rodrigues).

0927-7765/$ – see front matter © 2013 Elsevier B.V. All rights reserved.
http://dx.doi.org/10.1016/j.colsurfb.2013.03.050

polymerization (SI-ATRP) with a hydrophilic monomer, poly(ethylene glycol) methacrylate (PEGMA) for the hydrophilization of the surface of PDMS.

In recent years there has been a growing interest in surface-initiated polymerization reactions. The "grafting-from" approach has been favored as it allows tailoring the surface properties of the grafted materials to a high extent. This control can be achieved by a living/controlled radical polymerization process. From several possible approaches, SI-ATRP is a highly attractive one, owing its success to the wide variety of monomers, functionalities and experimental reaction conditions to which it is applicable. SI-ATRP is based on the reversible activation/deactivation between alkyl halides (R-X) by means of a metal catalyst complexed with ligands (Mt^n/2L). This dynamic equilibrium results in the formation of growing radicals ($R^\bullet$) that propagate by the addition of the monomer (M). Control is achieved by fast initiation relative to slower polymerization rates [18–22]. Therefore, SI-ATRP opens interesting possibilities to enhance PDMS surface functionality, especially the case of aqueous polymerization, which in contrast to the use of organic solvents, has a significant lower environmental impact. Furthermore, faster polymerization rates, higher molecular mass polymers, and high conversions can be obtained with this method [21]. Interestingly, despite its biomedical applications, few authors reported the successful polymerization by SI-ATRP on silicone rubber. In fact only five (and mostly recent) publications were found [23–27], in which Sylgard 184 (silicone rubber) was used as a model substrate for the surface polymerizations.

In the current work, SI-ATRP was used to prepare non-fouling PEGMA brushes onto silicone rubber. The surface was activated with 1-trichlorosilyl-2-(chloromethylphenyl)ethane (as an initiator) and further polymerized with PEGMA in aqueous media at room temperature. Copper was used as catalyst and 2,2′-bipyridine as ligand. The initiator was covalently bound to the surface by chemical vapor deposition. Physicochemical studies were conducted to characterize the modified surface (topography, hydrophilicity, functional groups, and elemental composition). *Staphylococcus aureus* GB 2/1 and *Streptococcus salivarius* GB 24/9 adhesion onto the modified surface was evaluated. Finally, human skin fibroblasts were cultured on modified PDMS to assess cell behavior and the absence of cytotoxicity.

2. Experimental

2.1. Materials

A silicone rubber sheet (ref. HT6240; 0.8 mm thickness) was a gift from *Stockwell Elastomerics, Inc.* (Philadelphia, PA, USA). The initiator 1-trichlorosilyl-2-(chloromethylphenyl)ethane (1-trichlorosilyl-2-CMPE) (94%, ref. T2455) was purchased from *United Chemical Technologies, Inc.* (Bristol, PA, USA). The monomer poly(ethylene glycol)methacrylate (PEGMA, Mw ≈ 360) was purchased from *Aldrich* (trademark of *Sigma–Aldrich Co. LLC*, registered in the USA and other countries) and 2,2′-bipyridyl (bpy, purity ≥ 98%) from *Fluka* (a trademark of *Sigma–Aldrich GmbH*, registered in the USA and other countries), Toluene (max. 0.005% H_2O) was supplied by *Panreac* (Barcelona, Spain), acetone (PA) by *Fisher* (Pittsburgh, PA, USA), copper (II) bromide (CuBr2) and copper (I) bromide (CuBr) by *Riedel-de Haën* (Hanover, Germany).

2.2. PDMS surface preparation and modification

The sequential experimental steps herein described were based on the works from Wu et al. [28], Xiao et al. [29], Li and Ruckenstein [30], Tugulu and Klok [27], with some modifications.

Surface modification of PDMS followed a three-step procedure (Fig. 1.). The first step (Fig. 1A) consisted of a surface hydroxylation by exposure of PDMS to ultraviolet light and ozone atmosphere (UVO), thus allowing the covalent attachment of hydroxyl groups on the materials' surface. This step was immediately followed by the covalent attachment of the initiator (1-trichlorosilyl-2-CMPE) to the hydroxylated PDMS surface (Fig. 1B) by a chemical vapor deposition technique. The activated surfaces were then surface polymerized by SI-ATRP (Fig. 1C) in aqueous media, at room temperature, using PEGMA as a monomer.

Samples exposed to UVO had an initial size of 2 cm × 9 cm. Following initiator attachment, samples were cut into 1 cm × 1 cm squares, and were individually used for the surface polymerization reactions.

2.2.1. Surface hydroxylation

UV/ozone (UVO) treatment (Fig. 1A) was done using a temperature controlled UV surface decontamination system (PSD-UVT, Novascan, Ames, IA, USA). This allows for the generation of atomic oxygen in a combination of photochemical processes: while the 185 nm line allows generating ozone from molecular oxygen, the 254 nm line converts ozone into atomic oxygen, which attacks the siloxane backbone of PDMS to form oxygen Si—OH surface structures [31]. PDMS samples were placed approximately at a 40 mm distance from the UV lamp and were treated for 10 min (for each side of the samples). The optimal exposure time was previously established based on the highest level of surface oxidation, while minimizing surface degradation. Surface oxidation (hydrophilization) was monitored by contact angle measurements (*data not shown*). In order to minimize the surfaces' hydrophobicity recovery, which is known to occur few hours after physical treatment [23,25], all surfaces (UVO-PDMS) were exposed to the initiator immediately after UVO hydrophilization.

2.2.2. Covalent attachment of the initiator

After UVO oxidation, each sample (UVO-PDMS, sizing 2 cm × 9 cm) was individually hanged with a string in a 500 mL flask containing 0.156 μL of initiator (I) per mm^2 sample surface area; the flask was then flooded with nitrogen, sealed with a stopcock and pumped to vacuum. Subsequently, each sealed flask was placed in an oil bath at 90 °C for 12 h (chemical vapor deposition of the initiator; Fig. 1B) [25]. Afterwards, the samples (I-PDMS) were removed from the flasks and the physically adsorbed initiator was removed from the surface by washing the samples for 2 min with toluene in an ultrasound bath, followed by 10 min with acetone and 20 min with distilled water [30,32]. All steps abovementioned were conducted at room temperature. The samples (I-PDMS) were then dried in an oven at 60 °C for 2 h, cut into 1 cm × 1 cm squares and kept in an excicator at room temperature until use.

2.2.3. Surface-grafting of PPEGMA brushes by ATRP

The surface polymerization with PEGMA (Fig. 1C) *via* SI-ATRP was performed according to the molar ratio of 110:5:1:10 of PEGMA:$CuBr_2$:CuBr:bpy. Prior to polymerization, 5 mL of distilled water with CuBr, $CuBr_2$, and bpy was bubbled with a nitrogen stream for 5 min. Next, 1 mL of PEGMA and a 1 cm × 1 cm sample (I-PDMS) was immediately added to the resulting brown reaction mixture. Each sample was polymerized individually. The reaction mixture was stirred at room temperature (20 °C) for up to 24 h, under inert atmosphere (nitrogen). At regular intervals the samples (PEGMA–PDMS) were removed from the solutions, washed in distilled water for 24 h to remove any unreacted monomer, catalyst and non-grafted material, dried at 60 °C, and stored in an excicator.

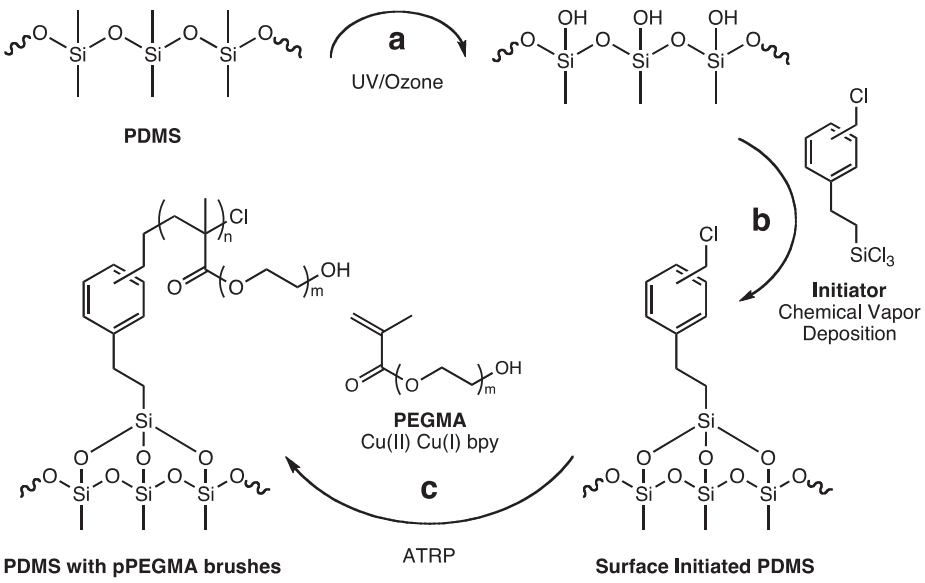

Fig. 1. Schematic representation of the surface-ATRP of PDMS. (a) UV/ozone activation of the PDMS surface. (b) Initiator attachment. (c) PEGMA polymerization onto PDMS by ATRP using Cu as a catalyst.

2.3. Physicochemical surface characterization

PDMS, before and following surface modification, was characterized using scanning electron microscopy (SEM), Fourier transform infrared spectroscopy in attenuated total reflection mode (FTIR-ATR), X-ray photoelectron spectroscopy (XPS), and by water contact angle measurements. Surface topography was evaluated at 300× magnification by SEM using a FEI Nova 200 equipment (EDAX Pegasus X4M). FTIR-ATR was performed using a Perkin-Elmer Spotlight 300 FTIR microscope with Spectrum 100 FTIR spectrometer. All spectra are averages of 100 scans measured at 4 cm^{-1} resolution. XPS spectra were recorded using a VG Scientific ESCALAB 200A equipped with PISCES software for data acquisition and analysis. An achromatic Al (Kα) X-ray source operating at 15 kV (300 W) was used and the spectrometer, calibrated with reference to Ag $3d_{5/2}$ (368.27 eV), was operated in CAE mode with 20 eV pass energy. Data acquisition was performed at a pressure lower then 10^{-6} Pa. Spectra analysis was performed using peak fitting with Gaussian–Lorentzian peak shape and Shirley type background subtraction (or linear according to the data). Advancing water contact angles were measured at room temperature using a Dataphysics OCA-20 drop shape analysis system (DataPhysics Instruments GmbH, Filderstadt, Germany) controlled by SCA20 software (drop size 3.0 μL). The reported contact angle values consisted of an average of three replicas, where in each, three measurements were taken.

2.4. Bacterial adhesion

S. aureus GB 2/1 and *S. salivarius* GB 24/9 were isolated from explanted voice prostheses [8] and were herein used as model organisms to study the effect of surface modification on their adhesion. The bacterial strains were first grown at 37 °C for 18 h in brain heart infusion broth (BHI, *OXOID*, England). Cells were then harvested by centrifugation for 5 min at 10,000 × *g*, washed twice with sterile demineralized water, and suspended in 200 mL phosphate buffer saline solution (PBS: 10 mM K_2HPO_4 plus 150 mM NaCl, pH 7.0) to a concentration of 3×10^8 bacteria mL^{-1}. A parallel plate flow chamber was used to study the deposition of bacteria under laminar flow as described elsewhere [33].

The parallel-plate flow chamber consists of a polymethylmethacrylate (PMMA) bottom plate with a thin sheet of PDMS (bare and modified) affixed to it with double sticky tape and a glass top plate, both with dimensions 5.5 cm × 3.8 cm. The top and bottom plates [33] were cleaned by sonicating for 3 min in a commercially available detergent solution (2% aqueous solution of Sonazol Pril, *Henkel Ibérica*, Alverca, Portugal), rinsed thoroughly with tap water, and then rinsed with demineralized water. Top and bottom plates were subsequently mounted in the housing of the flow chamber, separated by 0.06 cm spacers. Images were taken from the bottom plate, containing the bare or modified PDMS (three samples per condition), with a CCD video camera (SONY, Japan) mounted on a phase-contrast inverted microscope (Nikon, Diaphot) equipped with a 40× ultra-long working distance objective. The camera was coupled to an image analyzer (Image-Pro Plus 6.1, Media Cybernetics, Silver Spring, MD, USA). Each live image (768 × 576 pixels with 8-bit resolution) was obtained after summation of five consecutive images (time interval 500 ms) in order to enhance the signal-to-noise ratio and to eliminate moving bacteria from the analysis. Images were taken at different time intervals as follows: during the first 5 min images were taken every 30 s; from 5 to 25 min images were taken every minute; and during the last 3 h images were taken every 10 min.

Prior to each experiment, all tubes and the flow chamber were filled with PBS, during which care was taken to remove air bubbles from the system. Flasks, containing bacterial suspension and buffer, were positioned at the same height with respect to the chamber to ensure that immediately after the flows were started, all fluids would circulate (each fluid at the time) by hydrostatic pressure through the chamber at the desired shear rate of 10 s^{-1} (0.025 mL s^{-1}) that yields a laminar flow (Reynolds number 0.6). The microbial suspension was circulated through the system for 4 h and images were obtained from the bare or modified PDMS. The initial increase in the number of adhering bacteria with time was expressed in the so-called initial deposition rate j_0 (cm^{-2} s^{-1}), *i.e.* the number of bacteria adhering per unit area and time. The number of adhering microorganisms after 4 h was taken as an estimation of bacterial adhesion in a more advanced stage of the process. All values presented in this work are the averages of three separately bare or modified PDMS surfaces, and were carried out with separately grown microorganisms.

2.5. Cell-biomaterial interaction

The influence of the PEGMA coating in human skin fibroblasts (HSkF) (ATCC CRL-2429) cell growth and adhesion was evaluated *in vitro*. Bare PDMS surfaces were used as control. Cells were cultured in RPMI (Roswell Park Memorial Institute, GIBCO, UK) medium, supplemented with 10% FBS (fetal bovine serum, GIBCO, UK), 1% penicillin–streptomycin (GIBCO, UK) and 1% L-alanyl-L-glutamine (GlutaMAX-I, GIBCO, UK), at 37 °C in a humidified atmosphere of 95% air and 5% CO_2. The 1% PBS solution used was composed of 137 mM NaCl, 1.47 mM KH_2PO_4, 8.1 mM Na_2HPO_4, and 2.68 mM KCl (pH 7.4). For sub-culturing, 0.05% trypsin/EDTA (GIBCO, UK) was used.

PDMS samples were sterilized prior to cell culture using 70% (v/v) ethanol and 5 min of UV radiation (per sample side). Each sample was placed inside a well (1 cm × 1 cm square samples; four samples of bare and another four samples of modified PDMS) of a 12-well plate. Two 12-well plates were used for each incubation time tested, namely 48 and 120 h. In each well containing bare or modified PDMS samples, 6.7×10^4 cells were seeded and incubated. After each incubation time, cells were fixed for 5 min using 0.9 mL of 3.7% paraformaldehyde (PFA) in a buffer solution (pH 6.9) composed of 0.1 M PIPES (piperazine-N,N′-bis[2-ethanesulfonic acid]), 1 mM EGTA (ethylene glycol tetraacetic acid), and 4% (w/v) PEG 8000, then an extra 0.9 mL of PFA was added and left to react for 10 min. Afterwards, the PFA was removed and 1 mL of PBS was added; the plates were then wrapped up with aluminum foil and stored at 4 °C. Finally, cells from both plates were stained with fluorescent markers (as described in Section 2.5.1) and observed using confocal microscopy.

2.5.1. Immunocytochemistry

The immunocytochemistry assay was performed in two (out of four) wells for each type of surface. After fixation, 1 mL of 5% BSA (bovine serum albumin; *Sigma–Aldrich*) in PBS was added to each well for 30 min to block non-specific background. Then, 750 μL of the primary antibody diluted in PBSA (PBS + 1% BSA) was added to each well for 1 h, at 20 °C. Before incubating the secondary antibody each well was washed three times with 1 mL of PBSA. The secondary antibody, previously diluted in PBSA, was incubated for 1–2 h at 20 °C. Due to the presence of the fluorescent label the plates were covered up with aluminum foil during the incubations. Afterwards, the wells were washed four times for 5 min with 1 mL of PBSA and twice for 5 min with PBS. Then, the plates were again covered up with aluminum foil and were further observed using confocal microscopy. Two different primary antibodies were used, a polyclonal rabbit-anti-human fibronectin (1:400 dilution) and a monoclonal mouse-anti-human vinculin (1:100), in order to stain the fibronectin networks and the focal adhesions, respectively. Therefore, two secondary antibodies were used as well, namely a donkey-anti-rabbit IgG (immunoglobulin) with a redX (rhodamine) fluorescent label and a goat-anti-mouse IgG with a FTIC (fluorescein isothiocyanate) fluorescent label, both diluted 1:100. Both primary antibodies were purchased from *Sigma–Aldrich*. All secondary antibodies were purchased from *Jackson ImmunoResearch Europe Ltd.* (Suffolk, England). Finally, DAPI (4′,6-diamidino-2-phenylindole) was also added to stain the nuclei (4 μg mL^{-1}).

2.5.2. Confocal microscopy

The cells' conformation as well as fibronectin and vinculin expression was observed using a LEICA TCS SP2 (LEICA, Germany) confocal microscope. Pictures were taken at three distinct spots in each sample. Using the LEICA Software, confocal images stacks corresponding to several optical slices were taken. The thickness of each image stack was selected to include all the relevant structures. Two-dimensional projections were generated. For comparison purposes, the scale and resolution of all pictures was set to be the same. Each picture covered an area of 375 μm × 375 μm, corresponding to 1024 × 1024 pixels.

3. Results

3.1. Physicochemical surface characterization

Water contact angle measurements allowed evaluating the hydrophilization of PDMS surface following PEGMA SI-ATRP. Evolution of the PDMS surface with the polymerization time can be observed in Fig. 2 (following 0, 3, 6, 12 and 24 h of polymerization), whereby a progressive decrease in the surface hydrophobicity occurs with the polymerization, up to 24 h, with no further decrease in the water contact angle values afterwards (*data not shown*). Bare PDMS water contact angle was found to be 114.2 ± 1.4° which is in accordance with the values usually reported for silicone rubber surfaces [33]. Attachment of the initiator (I-PDMS), corresponding to 0 h (Fig. 2), was found to lower the contact angle to 94.2 ± 0.9°. This decrease may be ascribed to the free (unreacted) surface hydroxyl groups, following vapor deposition of the initiator (as observed bellow, by FTIR-ATR).

Following water contact angle determination PDMS samples were analyzed by SEM (Fig. 3) to assess if the initiator deposition (Fig. 3B) or the surface polymerization (Fig. 3C) affected the PDMS surface topography (Fig. 3A). Results show that, even after 24 h of polymerization, no detectable alteration of the PDMS surface could be observed (similar observations were recorded for the other polymerization times (*data not shown*)). Based on these results, in the following studies samples corresponding to the 24 h of polymerization were used.

Fig. 4 shows the results from FTIR-ATR spectra of the untreated (PDMS), surface-initiated (I-PDMS) and polymerized samples (PEGMA–PDMS). The peak at 2963 cm^{-1} from PDMS, corresponds to the stretching of CH_3 groups [17,23,24]. Attachment of the trichlorosilane initiator by vapor deposition (I-PDMS) does not change the spectra profile of PDMS, possibly due to the low degree of the substitution of the hydroxulated surface, following surface modification. Indeed (as observed bellow), the low percentage of Cl (0.7) as assessed by elemental composition (Table 1) further suggests the low surface substitution. Rather, a wide band (325–3750 cm^{-1}) corresponding to surface O—H stretch of silanols is evident, characteristic of surface oxidation by UVO

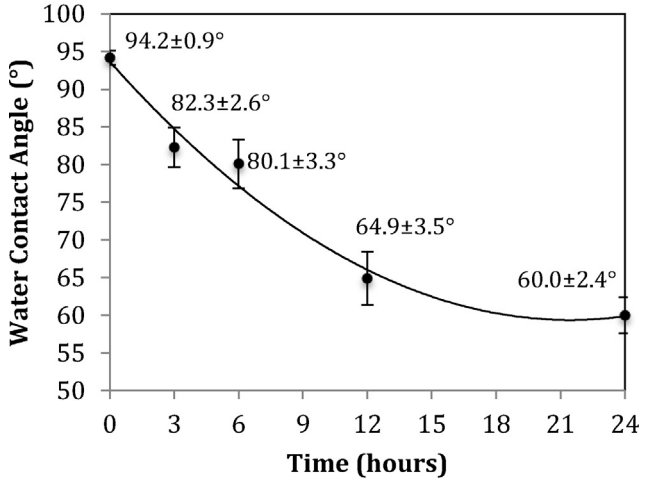

Fig. 2. Water contact angle values of PDMS–PEGMA surfaces at different polymerization times (0 h corresponds to a I-PDMS sample (see Section 2.2.2)). Standard error bars were calculated using Student's *t* distribution. Data were fitted by a second degree polynomial function to aid trend visualization.

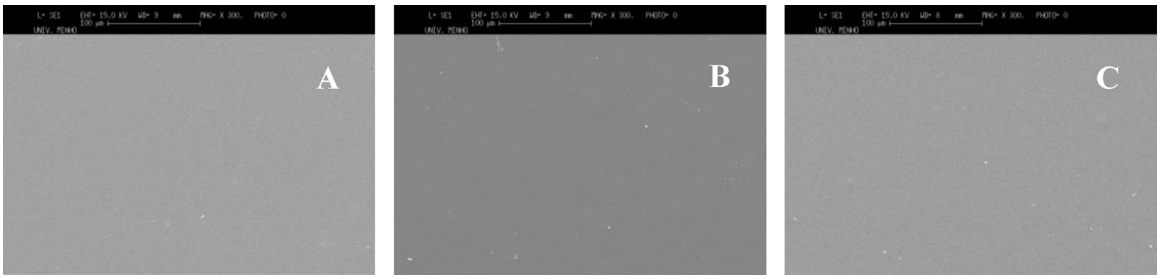

Fig. 3. SEM images from a bare (untreated) PDMS sample (A); following initiator attachment (I-PDMS; B) and after 24 h polymerization with PEGMA, *via* surface-ATRP (PEGMA–PDMS; C).

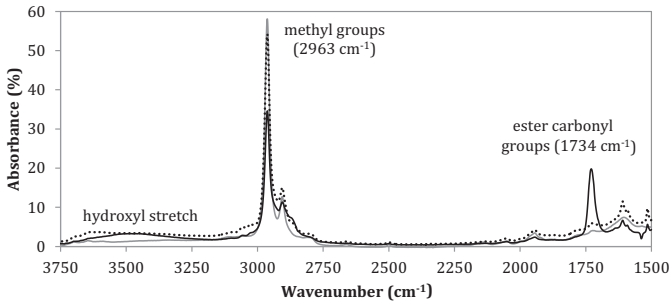

Fig. 4. FTIR-ATR spectra for PDMS (gray solid line), I-PDMS (dotted line) and PEGMA–PDMS (black solid line).

[30]. This suggests that, even after 12 h of initiator deposition, unreacted surface hydroxyl groups are present in PDMS. In surface-initiated ATRP, initiator concentration is usually much lower that used for solution ATRP. General approaches to allow establishing equilibrium between active and dormant chains during the polymerization, including the use of sacrificial initiator or additional deactivating species, to better control the polymerization [34]. Following PEGMA polymerization, the absorbance at 2963 cm^{-1} markedly drops; in parallel a peak at 1734 cm^{-1}, assigned to the ester's carbonyl group from PEGMA, is evident [27]. These results demonstrate that sufficient initiator sites were created by vapor deposition, to allow surface polymerization of PEGMA. Elemental composition (in percentage) of the PDMS samples is presented in Table 1, and the corresponding XPS wide spectra are illustrated in Fig. 5I. Each initiator molecule (1-trichlorosilyl-2-(chloromethylphenyl)ethane) has one silicium (Si), four chlorine (Cl), and nine carbon (C) atoms (Fig. 1.). During vapor deposition (see Section 2.2.2), the initiator binds to the —OH groups from the UVO treated PDMS (see Section 2.2.1) with the release of three HCl molecules for each attached initiator molecule. Therefore, after initiator deposition, all four elements (C 1s, O 1s, Si 2p and Cl 2p) are added to the surface's chemical composition. The occurrence of Cl in I-PDMS suggests the presence of the initiator at the surface of PDMS. By SI-ATRP polymerization, the initiator's Cl atoms are replaced by PEGMA monomer; thus a controlled sequential addition of the monomer results in PEGMA polymerization (Fig. 1). From Table 1 and XPS wide spectra (Fig. 5I) analysis, a decrease in the relative elemental composition of Si and Cl occurs with an increase in C and O from PEGMA polymerization. These results suggest (despite the low surface coverage of the initiator) the successful attachment of the initiator onto the PDMS surface followed by the successful formation of polyPEGMA (PPEGMA) brushes by surface SI-ATRP. Further, the occurrence of 0.2% Cl following PEGMA polymerization can be ascribed to living PEGMA chains. The reduction from 0.7 to 0.2% may indicate chain termination reactions may have occurred, which are expectable following high extents of polymerization. A similar behavior regarding low surface coverage by the initiator and possible termination reactions were observed by Xu et al. [35].

Table 1
Elemental composition (in %) of PDMS samples (bare (PDMS); following initiator attachment (I-PDMS) and following 24 h ATRP polymerization (PEGMA–PDMS)).

Sample	C 1s	O 1s	Si 2p	Cl 2p
PDMS	39.0	30.2	30.8	0.0
I-PDMS	44.1	28.3	26.9	0.7
PEGMA–PDMS	52.2	30.1	17.5	0.2

The carbon 1s (C 1s) spectra of PDMS and PEGMA–PDMS samples are illustrated in Fig. 5II. The peak located at 284.7 eV is associated with C—Si and C—H bonds. Grafted PEGMA shows two additional peaks related to the ether (—C—O—C—, 286.1–288.0 eV) and the ester carboxyl (O═C—O, 288.0–289.4 eV) groups [27,36,37]. The —C—O—C— ether peak may also contain another binding energy pertaining to a C—O group from PEGMA, the hydroxyl from —C—OH (at 286.4–286.7 eV). However, it was not visible possibly due to peak overlapping [37].

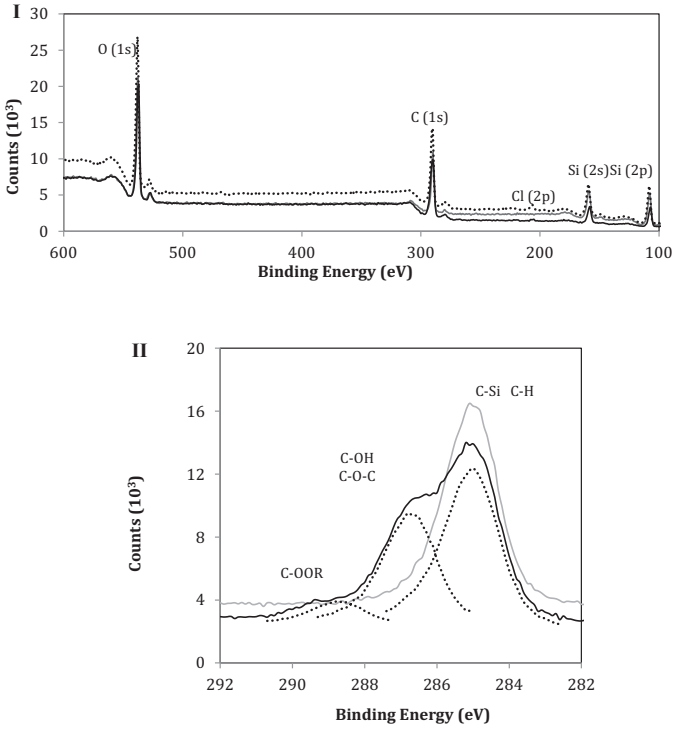

Fig. 5. XPS wide spectra for PDMS (gray solid line), I-PDMS (dotted line) and PEGMA–PDMS samples (black solid line) (Part I). C 1s core level regions spectrum for PDMS (gray solid line) and PEGMA–PDMS (black solid line). Polymerized PDMS spectrum decomposition is shown by dotted lines (Part II).

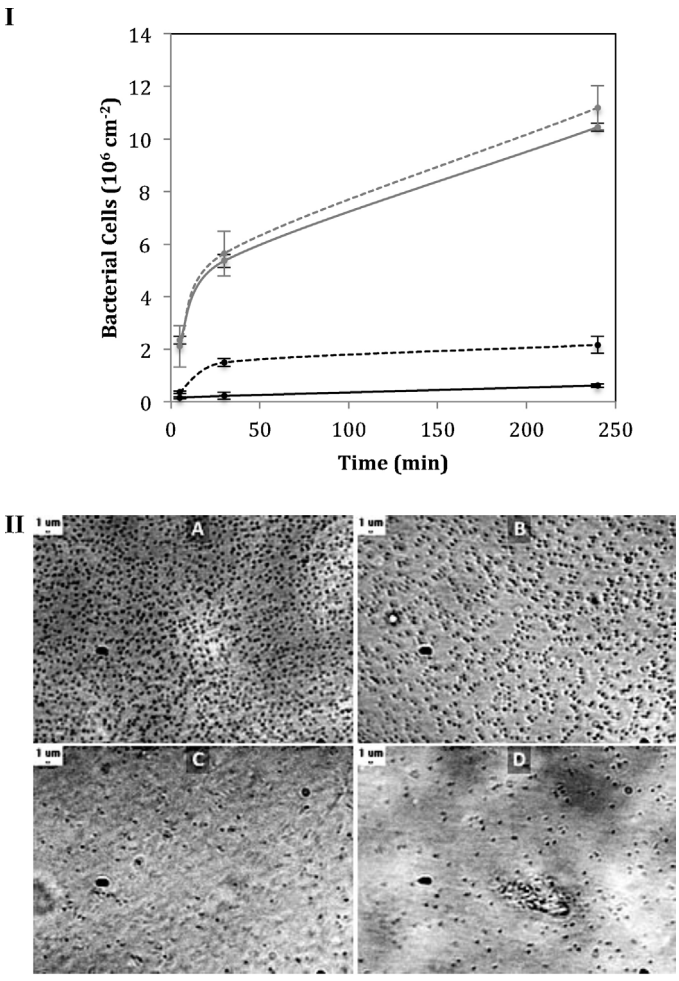

Fig. 6. Adhesion kinetics of *S. aureus* GB 2/1 (continuous lines) and *S. salivarius* GB 24/9 (dotted lines) onto PDMS (gray lines) and PEGMA–PDMS (black lines) (Part I). Bacterial adhesion onto PDMS surfaces after 4 h: *S. aureus* GB 2/1 (A and C) and *S. salivarius* GB 24/9 (B and D) adhesion onto PDMS (A and B) and PEGMA–PDMS (C and D). Images were acquired using a 40× ultra long working distance objective (Part II).

3.2. Bacterial adhesion

Fig. 6I illustrates the adhesion kinetics of *S. aureus* GB 2/1 and *S. salivarius* GB 24/9 to bare PDMS and PEGMA–PDMS. A reduction in bacterial adhesion onto polymerized PDMS surfaces was found for both strains, compared to the control. Initial deposition rates for *S. aureus* GB 2/1 and *S. epidermidis* GB 24/9 onto bare PDMS were $2067 \pm 59\,cm^{-2}\,s^{-1}$ and $2333 \pm 62\,cm^{-2}\,s^{-1}$, respectively. After modifying the surface with PEGMA brushes, the adhesion was found to be around 5-fold slower ($433 \pm 43\,cm^{-2}\,s^{-1}$) for *S. aureus* GB 2/1, and 3-fold slower for *S. epidermidis* GB 24/9 ($733 \pm 67\,cm^{-2}\,s^{-1}$).

Furthermore, the numbers of bacterial adhesion adhering after 4 h were found to decrease. Reductions of 94.1% and of 80.6% were found for *S. aureus* GB 2/1 and *S. salivarius* GB 24/9, respectively. The same trend can be qualitatively observed in Fig. 6II, which illustrates bacterial adhesion onto PDMS and PEGMA–PDMS surfaces after 4 h of contact.

3.3. Cell-biomaterial interaction

Imaging the cell-biomaterial interactions using immunocytochemical staining can provide significant information about cell phenotype and function. The confocal microscopy images obtained from bare and modified PDMS samples seeded with fibroblasts for two distinct time points (48 and 120 h) are illustrated in Fig. 7. More cells have adhered to the bare PDMS (Fig. 7A and B) than to PEGMA–PDMS (Fig. 7C and D) for the first time point. However, after 120 h, the modified samples showed higher surface coverage with an organization consisting of cells with a stretched conformation, suggesting that these surfaces are a better substrate for fibroblast adhesion and differentiation. Furthermore, these results suggest that the modified PDMS surface does not present any cytotoxicity issue.

4. Discussion

We have used atom-transfer radical-polymerization for the surface polymerization of PEGMA monomers on PDMS surfaces, in aqueous media, at room temperature. Water was needed as a solvent, given that, when using PEGMA alone, the surface of the PDMS buckled, a phenomenon also observed by Edmondson et al. [38]. Under aqueous media, the PEGMA–PDMS were shown to be endowed with a hydrophilic character, which allowed a significant reduction of bacterial adhesion of two strains commonly found in silicone rubber prosthetic devices (*S. aureus* GB 2/1 and *S. salivarius* GB 24/9) [39]. PDMS can be used in a wide range of prosthetic devices that are subjected to very different surrounding media, nevertheless in the current study we used PBS since we were not targeting a specific device and therefore it is a good compromise to mimic physiological serum. For studying bacterial adhesion to a specific device a more adequate media mimicking its conditions is recommended.

Preventing or retarding biofilm formation in prosthetic devices is of major importance when engineering novel materials for biomedical applications [11]. This often implies that it is necessary to interfere in the weakest link, which means in the formation of the conditioning film (*i.e.* protein nonspecific adsorption to the material surface) and adhesion of the first bacteria. Both studied bacteria are hydrophilic and normally an organism will tend to adsorb irreversibly to minimize the free energy of the system. However, charge repulsion or steric exclusion may prevent close approach, and even when this has been achieved, ordered water structure associated very closely with the surface could still be a barrier [33]. Hydrophilic surfaces may be stabilized by ordering of surface-associated water molecules, which would be disrupted by the close approach of bacterial cell. This releases the ordered water molecules into the bulk phase, increasing their free energy. Therefore, it was expected that making the surface of PDMS more hydrophilic would result in a reduction of bacterial adhesion. It is important to notice that, although around 1×10^6 cells cm^{-2} adhered at the modified surfaces after 4 h, one log reduction of bacterial adhesion could be found for both strains compared to the unmodified surfaces. Therefore, such PDMS surface modification by decreasing the initial bacterial adhesion will further delay biofilm formation and eventually the occurrence of infection. As previously mentioned, preventing or reducing bacterial adhesion in the first hours upon implantation of a device is crucial for its long-term success. The hydrophilic character of PDMS further increased following PEGMA polymerization (contact angle of $60 \pm 2.4^\circ$, Fig. 2), as compared to a UVO treated and initiator deposited sample (contact angle of $94.2 \pm 0.9^\circ$). FTIR-ATR analysis suggests that, given the availability of surface OH groups, following initiator deposition, the reaction was not complete (even after 12 h vapor deposition). This also indicates that with the vapor deposition technique, a fraction of the initiator is indeed only physically adsorbed onto PDMS and is removed from the surface following subsequent washing.

The anti-adhesive effect of PDMS grafted PEGMA may be ascribed to the large excluded volume by its chains and their mobility and flexibility in aqueous media, preventing cells from

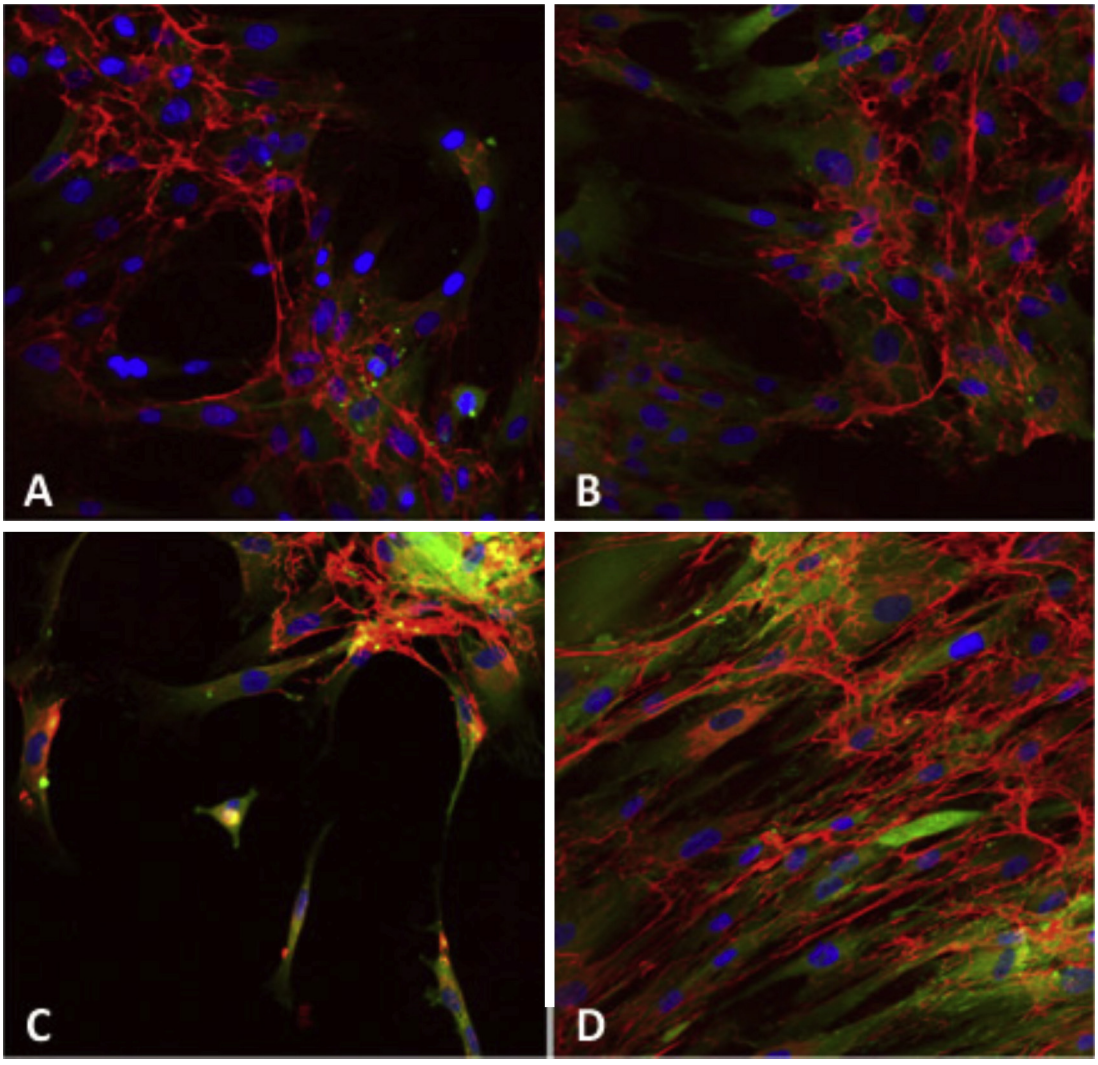

Fig. 7. Confocal microscopy images of the immunochemistry assay conducted after exposing fibroblasts to PDMS (A and B) and PEGMA–PDMS (C and D) for 48 (A and C) and 120 h (B and D). The green staining represents vinculin, a structural protein present in the cytoplasmic side of focal adhesions. Fibronectin stains red and cell nuclei, blue. (For interpretation of the references to color in this figure legend, the reader is referred to the web version of the article.)

approaching the substrate's surface, hence impeding microbial adhesion [11,22].

PEGMA is not an antimicrobial so no killing is expected due to this modification. On contrary, being a hydrophilic polymer it is expected to modify the physicochemical properties of the PDMS substrate. Several researchers have been using PEGMA for this type of strategies (*e.g.* [40,41]). In the current work, further indication of PEGMA polymerization onto PDMS was obtained by XPS analysis whereby the peaks related to the ether —C—O—C— and the ester carboxyl O═C—O group from PEGMA were identified.

Under the assayed conditions, the topography of the PDMS surface was preserved (as observed by SEM), while increasing its hydrophilicity, as observed from the decrease in the water contact angles measured (Fig. 2).

Furthermore, cell morphology and distribution on the biomaterial surface were assessed not only to evaluate the cells interaction with the biomaterial but also to identify a possible substratum cytotoxic effect. The results obtained from *in vitro* studies with human skin fibroblasts showed slower initial fibroblast adhesion onto the PEGMA–PDMS. This would be expected given the steric hindrance caused by the PEGMA chains that can prevent adequate adsorption of (adhesive) proteins. Contrarily, the faster short-term fibroblasts adhesion to bare PDMS is associated to the PDMS hydrophobic nature, which makes it more prone to protein adsorption (the first step in the adhesion phenomena), even if the composition of the adsorbed protein layer is not optimal for cell adhesion. With all samples assembled fibronectin fibers were detected, which became organized into networks with increasing density over time, characteristic of a good cell attachment onto PDMS [42]. Vinculin can also be observed, but focal adhesions (patches containing vinculin) present at 48 h are limited. Vinculin and fibronectin were both co-localized after 120 h, and are associated with focal adhesions. This was observed in both bare and modified PDMS surfaces although for the modified surface the density of the network is higher. Therefore, these results suggest that the modified PDMS allows better fibroblast differentiation and it presents no pronounced cytotoxic effect.

5. Conclusions

This work focused on the chemical and biological characteristics of PDMS modified by surface initiated ATRP of PEGMA, in aqueous media at room temperature. The modification process allowed for a decrease in the surface hydrophobicity, while preserving the surface topography. Bacterial adhesion was significantly decreased on the hydrophilized surfaces.

Human skin fibroblasts showed higher adhesion on the PEGMA–PDMS samples. The results show that this modification is a promising approach to reach a more generalized use of a material that is already extensively used for manufacturing implantable medical devices.

Acknowledgments

The authors acknowledge Stockwell Elastomerics Inc. for kindly proving the silicone rubber samples (ref. HT6240). SEM, FTIR-ATR and XPS studies were performed at SEMAT (University of Minho, Portugal), DEP (University of Minho, Portugal) and CEMUP (University of Porto, Portugal) facilities, respectively. Also, the authors acknowledge the financial support from Fundação para a Ciência e Tecnologia (FCT) to the project BIOSURFA – Application of biosurfactants for microbial adhesion inhibition in medical devices (PTDC/SAU-BEB/73498/2006).

References

[1] M. Waters, R. Jagger, G. Polyzois, J. Prosthet. Dent. 81 (1999) 439.
[2] U.S. Maller, K. Karthik, S.V. Maller, J. Ind. Acad. Dental. Spec. 1 (2010) 25.
[3] V.A. Chalian, R.W. Phillips, J. Biomed. Mater. Res. 8 (1974) 349.
[4] G. Polyzois, R. Winter, G. Stafford, Biomaterials 12 (1991) 79.
[5] P. Zilla, D. Bezuidenhout, Biomaterials 28 (2007) 5009.
[6] N.P. Boks, W. Norde, H.C. van der Mei, H.J. Busscher, Microbiology 154 (2008) 3122.
[7] C. Bower, J. Parker, A. Higgins, M. Oest, J. Wilson, B. Valentine, M. Bothwell, J. McGuire, Coll. Surf. B: Biointerfaces 25 (2002) 81.
[8] L.R. Rodrigues, I.M. Banat, J.A. Teixeira, R. Oliveira, J. Biomed. Mater. Res. B 81 (2007) 358.
[9] A.G. Gristina, Science 237 (1987) 1588.
[10] K.A. Poelstra, N.A. Barekzi, A.M. Rediske, A.G. Felts, J.B. Slunt, D.W. Grainger, J. Biomed. Mater. Res. 60 (2002) 206.
[11] L.R. Rodrigues, in: D. Linke, A. Goldman (Eds.), Bacterial Adhesion: Biology, Chemistry and Physics, Series Advances in Experimental Medicine and Biology, vol. 715, Springer, Germany, 2011.
[12] F. Abbasi, H. Mirzadeh, A. Katbab, Polym. Int. 50 (2001) 1279.
[13] P. Hron, Polym. Int. 52 (2003) 1531.
[14] K.Y. Lee, W.S. Ha, W.H. Park, Biomaterials 16 (1995) 1211.
[15] S. Sofia, E. Merill, J. Harris, S. Zalipsky (Eds.), Poly(ethylene glycol): Chemistry and Biological Applications, American Chemical Society, Washington, DC, 1997.
[16] L.R. Rodrigues, H.C. van der Mei, I.M. Banat, J.A. Teixeira, R. Oliveira, FEMS Immunol. Med. Microbiol. 46 (2006) 107.
[17] S. Pinto, P. Alves, A.C. Santos, C.M. Matos, B. Oliveiros, S. Gonçalves, E. Gudiña, L.R. Rodrigues, J.A. Teixeira, M.G. Gil, J. Biomed. Mater. Res. A 98 (2011) 535.
[18] D. Bontempo, N. Tirelli, K. Feldman, G. Masci, V. Crescenzi, J.A. Hubbell, Adv. Mater. 14 (2002) 1239.
[19] K. Matyjaszewski, J. Xia, Chem. Rev. 101 (2001) 2921.
[20] K. Matyjaszewski, J. Spanswick, Mater. Today 8 (2005) 26.
[21] J. Qiu, B. Charleux, K. Matyjaszewski, Prog. Polym. Sci. 26 (2001) 2083.
[22] F.J. Xu, K.G. Neoh, E.T. Kang, Prog. Polym. Sci. 34 (2009) 719.
[23] I. Fundeanu, H.C. van der Mei, A.J. Schouten, H.J. Busscher, Coll. Surf. B: Biointerfaces 64 (2008) 297.
[24] I. Fundeanu, D. Klee, A.J. Schouten, H.J. Busscher, H.C. van der Mei, Acta Biomater. 6 (2010) 4271.
[25] D. Xiao, H. Zhang, M. Wirth, Langmuir 18 (2002) 9971.
[26] Z. Jin, W. Feng, S. Zhu, H. Sheardown, J.L. Brash, J. Biomater. Sci. Polym. 21 (2010) 1331.
[27] S. Tugulu, H.-A. Klok, Macromol. Symp. 279 (2009) 103.
[28] T. Wu, K. Efimenko, J. Genzer, Macromolecules 34 (2001) 684.
[29] D. Xiao, M.J. Wirth, Macromolecules 35 (2002) 2919.
[30] Z.F. Li, E. Ruckenstein, J. Colloid Interface Sci. 251 (2002) 343.
[31] D. Bodas, C. Khan-Malek, Microelectron. Eng. 83 (2006) 1277.
[32] S. Tugulu, P. Silacci, N. Stergiopulos, H.-A. Klok, Biomaterials 28 (2007) 2536.
[33] L.R. Rodrigues, H.C. van der Mei, J.A. Teixeira, R. Oliveira, Appl. Microbiol. Biotechnol. 66 (2004) 306.
[34] K.M. Matyjaszewski, P.J. Miller, N. Shukla, B. Immaraporn, A. Gelman, B.B. Luokala, T.M. Siclovan, G. Kickelbick, T. Vallant, H. Hoffmann, T. Pakula, Macromolecules 32 (1999) 8716.
[35] F.J. Xu, Z.H. Wang, W.T. Yang, Biomaterials 31 (2004) 3139.
[36] X. Zou, E. Kang, K. Neoh, Plasmas Polym. 7 (2002) 151.
[37] S. Pinto, P. Alves, C.M. Matos, A.C. Santos, L.R. Rodrigues, J.A. Teixeira, M.H. Gil, Coll. Surf. B: Biointerfaces 81 (2010) 20.
[38] S. Edmondson, K. Frieda, J.E. Comrie, P.R. Onck, W.T.S. Huck, Adv. Mater. 18 (2006) 724.
[39] N. Ariani, A. Vissink, R.P. van Oort, L. Kusdhany, A. Djais, T.B.W. Rahardjo, H.C. van der Mei, B.P. Krom, Biofouling 28 (2012) 583.
[40] D. Xu, W.H. Yu, E.T. Kang, K.G. Neoh, J. Colloid Interface Sci. 279 (2004) 78.
[41] F.J. Xu, S.P. Zhong, L.Y.L. Yung, E.T. Kang, K.G. Neoh, Biomacromolecules 5 (2004) 2392.
[42] T.G. van Kooten, H.T. Spijker, H.J. Busscher, Biomaterials 25 (2004) 1735.